Article

Not peer-reviewed version

Psoralen and Isopsoralen from *Psoralea corylifolia* Suppress NSCLC by Dual Mechanisms: STAT3 Inhibition and ROS Modulation

Liwei Bi , Guangyi Chen , Wanfen Liu , Anastacio T. Cagabhion , Yu-Wei Chang , Zhengyuan Yao , Jing Feng , Yi Liu , Siyi Chen , Yung-Husan Chen *

Posted Date: 23 December 2025

doi: 10.20944/preprints202512.1925.v1

Keywords: STAT3; *Psoralea corylifolia*; SPR; NSCLC; ROS

 doi:10.20944/preprints202512.1925.v1

Article

Psoralen and Isopsoralen from *Psoralea corylifolia* Suppress NSCLC by Dual Mechanisms: STAT3 Inhibition and ROS Modulation

Liwei Bi [1,2,3], Guangyi Chen [1], Wanfen Liu [1], Anastacio T. Cagabhion III [4,5], Yu-Wei Chang [4], Zhengyuan Yao [6], Jing Feng [1], Yi Liu [1] and Siyi Chen [1], Yung-Husan Chen [1,2,3,*]

[1] Department of Pharmacy, Xiamen Medical College, Fujian Province, Xiamen 361023, China
[2] Fujian Provincial University Engineering Research Centre for Marine Biomedical Resources, Xiamen Medical College, Xiamen 361023, China
[3] Xiamen Key Laboratory of Natural Products Resources of Marine Medicine, Xiamen Medical College, Xiamen 361023, China
[4] Department of Food Science, National Taiwan Ocean University, Keelung 20224, Taiwan
[5] Department of Home Economics, Western Philippines University, San Juan, Aborlan 5302, Philippines
[6] Department of Basic Medicine, Xiamen Medical College; Xiamen 361023, China
* Correspondence: cyxuan@xmmc.edu.cn

Abstract

Non-small cell lung carcinoma (NSCLC) is the most prevalent form of lung cancer, and its progression is strongly driven by the constitutive activation of signal transducer and activator of transcription 3 (STAT3). This study used surface plasmon resonance (SPR) technology to develop a STAT3-targeting recognition system and identify natural inhibitors from the traditional Chinese medicine *Psoralea corylifolia*. SPR analysis showed that psoralen and isopsoralen bind effectively to STAT3, with equilibrium dissociation constants (KD) of 80.92 μM and 28.11 μM, respectively. Molecular docking further confirmed their interaction with the STAT3 SH2 domain. Beyond direct STAT3 inhibition, both compounds demonstrated notable free radical scavenging activity. In a hydrogen peroxide (H_2O_2)-induced oxidative stress model, pretreatment with psoralen or isopsoralen significantly reduced reactive oxygen species (ROS) levels in human umbilical vein endothelial cells (HUVECs), while increasing ROS accumulation in A549 lung cancer cells. This combined ability to inhibit STAT3 and regulate redox homeostasis underlies their anti-NSCLC effects, including strong suppression of cancer cell proliferation and migration. Importantly, neither compound exhibited significant cytotoxicity in normal cells, indicating favorable selectivity. This work identifies psoralen and isopsoralen as novel dual-function STAT3 inhibitors and demonstrates the utility of SPR for screening bioactive natural products for targeted NSCLC therapy.

Keywords: STAT3; *Psoralea corylifolia*; SPR; NSCLC; ROS

1. Introduction

Lung cancer stands as the primary driver of global cancer mortality. According to global statistics, approximately 1.8 million individuals succumbed to lung cancer in 2022 [1]. Non-small cell lung cancer (NSCLC) constitutes roughly 85% of all lung carcinoma diagnoses [2]. Notably, nearly two-thirds of NSCLC cases are identified at advanced stages, resulting in a 5-year net survival rate of only 15-30% [3]. Targeted therapies, especially epidermal growth factor receptor tyrosine kinase inhibitors (EGFR-TKIs), have revolutionized outcomes for patients harboring specific driver mutations. However, their long-term effectiveness is limited by several key challenges: restricted indications, treatment-related toxicities and adverse effects, and the inevitable emergence of acquired resistance [4,5]. Platinum-based chemotherapy remains the standard of care for patients lacking

 doi:10.20944/preprints202512.1925.v1

actionable driver mutations (approximately 50% of NSCLC cases), underscoring the urgent need to develop novel antitumor agents with high efficacy and low toxicity [6].

Signal transducer and activator of transcription 3 (STAT3) regulates genes involved in cellular physiopathological processes. STAT3 is constitutively activated in more than 50% of NSCLC patients [7]. As a critical driver of multiple cancers, aberrantly activated STAT3 plays a pivotal role in promoting tumorigenesis, drug resistance, and metastasis in NSCLC, with multidimensional regulatory mechanisms underlying its oncogenic activity [3]. STAT3 can be phosphorylated and activated by the Janus kinase family to upregulate anti-apoptotic proteins (e.g., Bcl-xL and Mcl-1), cell-cycle regulators (e.g., cyclin D1 and c-Myc), and vascular endothelial growth factor (VEGF) expression, thereby promoting tumor proliferation, survival, and angiogenesis [8]. Additionally, STAT3 encourages the expansion of myeloid-derived suppressor cells (MDSCs), inducing immunosuppression in lung cancer [9]. High STAT3 activation in the tumor microenvironment promotes the expression of epithelial-to-mesenchymal transition (EMT)-related transcription factors, including Snail, Twist, and ZEB1, which drive cancer metastasis by upregulating genes involved in metastasis [10]. Cisplatin remains the primary chemotherapeutic agent for advanced NSCLC treatment; STAT3 expression is closely associated with tumor cell sensitivity to chemotherapeutic agents. Inhibiting STAT3 activity or expression can enhance tumor cell sensitivity to chemotherapeutic agents such as cisplatin, thereby improving treatment outcomes [11]. Consequently, discovering new drugs with STAT3-inhibitory activity is crucial to improving NSCLC therapy. No direct STAT3 inhibitors have been approved for marketing and are under preclinical and clinical studies. Most small molecules (e.g., the imidazopyridine analogue W2014-S) can inhibit STAT3 dimerization or phosphorylation, but they suffer from insufficient selectivity and off-target effects [12,13]. Natural products have become a revolutionary trend in the development of anti-cancer drugs due to their multi-purpose regulatory properties and low toxicity. However, existing studies (e.g., on resveratrol and berberine) lack direct evidence of target binding [14].

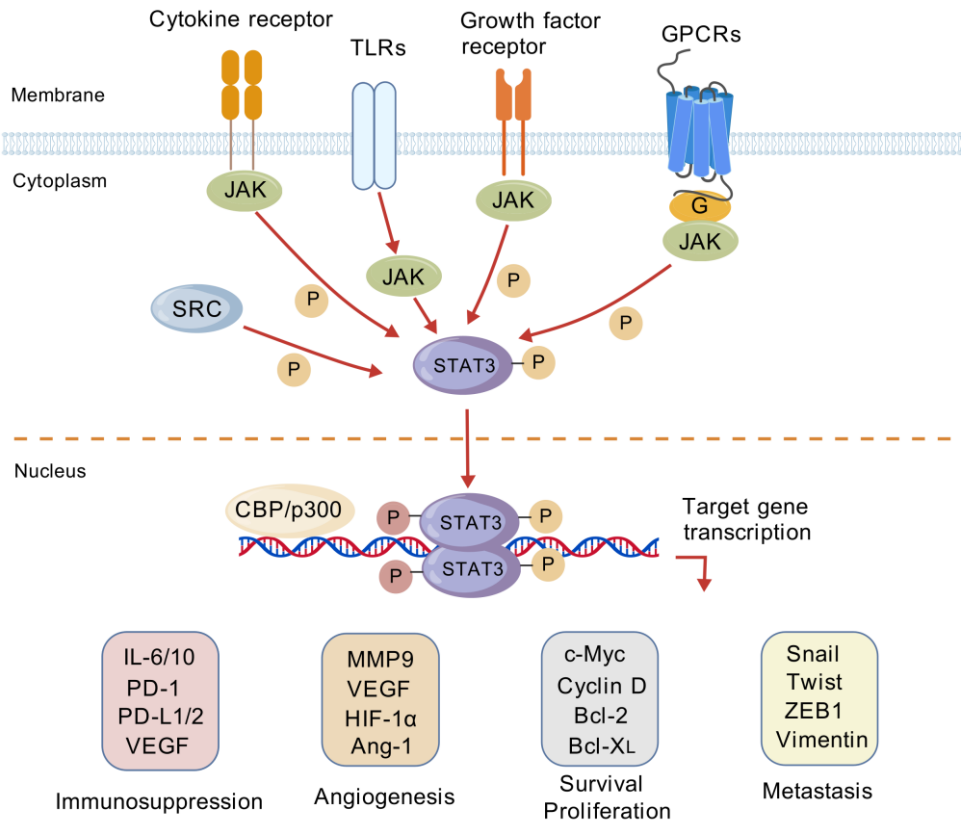

Figure 1. STAT3 signaling pathway in tumorigenesis and progression.

 doi:10.20944/preprints202512.1925.v1

Surface Plasmon Resonance (SPR) biosensors facilitate real-time, label-free monitoring of biomolecular interactions, especially in characterizing small molecule-protein binding events (e.g., determining affinity and dissociation constants) [15]. This technology has demonstrated advantages, including label-free detection, real-time monitoring capability, and high specificity. Currently, SPR technology finds essential applications in research on active ingredients derived from traditional Chinese medicine (TCM) [16]. Notably, this technique eliminates the need to pre-separate components in herbal extracts, allowing direct screening of active ingredients that interact with specific target proteins. When combined with UPLC-Q-TOF-MS/MS, it enables accurate structural characterization of binding components. Compared to conventional SPR screening methods, the SPR-automated injection and retrieval system (SPR-AIRS) offers significant advantages, including higher detection throughput, enhanced enrichment capacity, and more definitive structural information [17].

Psoralea corylifolia Linn., also known as" Fructus Psoraleae" or "Bu Gu Zhi", refers to the dried fruits of this leguminous medicinal plant. As a traditional Chinese medicine (TCM), its earliest recorded mention appears in the ancient text "Lei Gong Pao Zhi Lun" (Eastern Han Dynasty) and was formally included in the "Tang Ben Cao" (Tang Dynasty) [18]. Its nature is pungent and bitter, warm in property, and it targets the kidney and spleen meridians. It is primarily used to treat conditions such as kidney yang deficiency-induced lumbago and knee cold pain, spermatorrhea, nocturia, frequent urination, the five fatigues and seven injuries, wind-cold disorders, and bone marrow injuries [19]. Additionally, it is widely used to manage vitiligo (leukoderma), psoriasis, and other skin conditions [20,21]. The primary chemical constituents of *Psoralea corylifolia* include coumarins, monoterpene phenols, flavonoids, and benzofuranes. Contemporary pharmacological studies have revealed that extracts and monomer compounds from *Psoralea corylifolia* possess unique therapeutic effects against infectious diseases, inflammatory disorders, tumors, and depression [22,23]. Recent findings indicate that the active compounds of *Psoralea corylifolia* demonstrate significant inhibitory and therapeutic effects on malignant tumor cells, including hepatocellular carcinoma [23], breast cancer [24], prostate cancer [24], colorectal cancer [25], gastric cancer [26], and lung cancer [27]. This echoes the aberrant STAT3 activation observed in malignant tumors. Current research has also primarily focused on the regulation of classical pathways, such as epidermal growth factor receptor (EGFR), by *Psoralea corylifolia* components. In contrast, the direct mechanistic intervention on the STAT3 signaling pathway remains unclear [28]. Investigating whether small molecules from *Psoralea corylifolia* exert antitumor effects by targeting STAT3 could not only deepen research on TCM modernization but also provide novel strategies for developing natural-origin STAT3 inhibitors [29].

Given the critical role of STAT3 in NSCLC, this study will use the SPR-AIRS system to identify small-molecule ligands targeting STAT3 proteins from *Psoralea corylifolia*. This study will simulate the binding mode of compounds to the SH2 domain through molecular docking and investigate the inhibitory effects of target compounds on NSCLC using cellular assays. This approach aims to provide novel ideas for developing natural-source STAT3 inhibitors and to establish a research paradigm for targeted screening of natural active ingredients.

Reactive oxygen species (ROS) are critically involved in the progression of multiple cancer types, across various malignancies, particularly by driving tumorigenesis through oxidative damage to intracellular lipids, proteins, and DNA, which can lead to genomic instability [30]. Within the tumor microenvironment, elevated ROS levels function as signaling molecules to activate oncogenic pathways (e.g., the ERK signaling pathway), thereby promoting cancer cell proliferation, angiogenesis, and metastasis [31]. Additionally, ROS exhibit a complex regulatory relationship with STAT3, acting as upstream activators that modulate STAT3 signaling [32]. Based on this framework, we hypothesize that the anti-NSCLC activity of compounds derived from *Psoralea corylifolia* may extend beyond direct STAT3 binding to encompass antioxidant mechanisms. Therefore, this study aims to investigate their direct inhibitory effects on STAT3 and to evaluate their potential antioxidant properties, thereby constructing a comprehensive understanding of their mechanism of action against NSCLC. The experimental flow is depicted in Figure 2.

 doi:10.20944/preprints202512.1925.v1

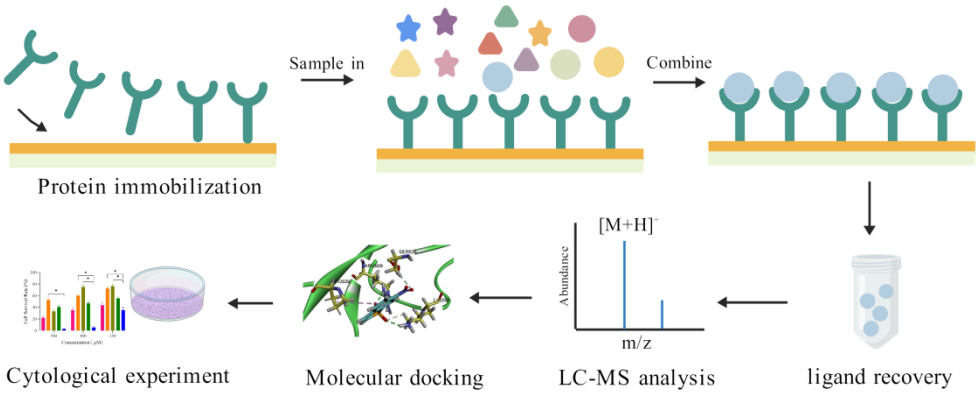

Figure 2. The screening process for targeted inhibitors derived from natural products.

Materials and Methods

2.1. Major Materials

STAT3 protein was ordered from AstraZeneca (China). CM5 microarray, amino-coupling kit, 50 mM sodium hydroxide solution, glycine hydrochloride (pH 3.0), and sodium acetate (pH 4.0) were obtained from GE Healthcare (USA). *Psoralea corylifolia*, a traditional *Chinese medicine*, was provided by Associate Prof. Wang Qing from the Xiamen Key Laboratory of Traditional Chinese Medicine Bioengineering. Psoralen and isopsoralen standards were ordered from Orileaf (Shanghai, China). Ammonium bicarbonate was purchased from Merck Sigma Corporation (USA). NSCLC cells (A549), human umbilical vein endothelial cells (HUVECs), and RAW264.7 cell lines were obtained from the Chinese Academy of Sciences (CAS) Cell Bank (Shanghai, China). The Cell Proliferation-Toxicity Assay Kit (CCK-8) was purchased from Biosharp (Anhui, China). Stattic was ordered from TargetMol (Shanghai, China). The ROS assay kit was ordered from Beyotime (Shanghai, China).

2.2. STAT3 Protein Immobilization

SPR was performed on a Biacore T200 system (GE Healthcare, USA) to immobilize STAT3 onto a CM5 sensing chip surface using the standard amine coupling protocol, with channels 2 or 4 serving as the detection pathway for STAT3 protein coupling. Initially, a 1:1 mixture of 1-ethyl-3-(3-dimethylaminopropyl) carbodiimide (EDC) and N-hydroxysuccinimide (NHS) was introduced at a flow rate of 10 μL/min for 10 min to activate the carboxyl groups on the dextran matrix surface. Subsequently, the STAT3 protein prepared at 50 μg/mL in 10 mM Acetate buffer (pH 4.0) was delivered at 10 μL/min for 7 min to facilitate covalent conjugation. Finally, residual active groups were blocked by injecting ethanolamine. The immobilization level was quantified by measuring the bound Response Units (RU).

2.3. STAT3 Protein Chip Specificity Examination

To validate the reliability of the experimental system, Stattic - a well-characterized small-molecule inhibitor of STAT3 was employed as a positive control [30]. At the same time, phosphate-buffered saline (PBS) served as the negative control. A serial dilution of Stattic was prepared in running buffer, and the kinetics/affinity experimental template was selected for affinity measurements. The Stattic concentration gradient was then analyzed with the following parameters: 60 s injection time, 30 μL/min flow rate, and 60 s dissociation time at 25 °C. The binding signals were specifically analyzed using reference-channel subtraction and blank subtraction. Data were fitted to a 1:1 steady-state affinity model, from which the equilibrium dissociation constants (KD) were directly derived to characterize the binding affinity between Stattic and STAT3 protein.

 doi:10.20944/preprints202512.1925.v1

2.4. Preparation and Screening of Psoralea corylifolia Extract

Psoralea corylifolia was crushed and passed through a 40-mesh sieve. One gram of the powder was weighed and separately extracted with 10 mL of either 60% or 90% ethanol using ultrasonic extraction for 30 min. The extracts were then filtered through 0.22 μm syringe filters. Each filtered extract was diluted with running buffer and centrifuged to obtain the supernatant. The Biacore T200 software system was launched, and the manual mode was selected. Then, *Psoralea corylifolia* extract was injected over the sensor chip surface for an association phase of 60 s, followed by a dissociation phase of 60 s, and then regenerated for 60 s. PBS buffer was injected between sample injections as a negative control to determine specific binding of the extract to immobilized STAT3 protein.

2.5. Recovery of Active Ingredients Bound to STAT3 Protein

The Biacore T200 software system was used, and channels 1-4 were selected. The CM5 chip was used, and STAT3 protein was immobilized simultaneously on the chip surface across all four channels. The flow rate was then set to 10 μL/min and the binding time to 420 s. Sample angling experiments were performed using the "inject and recover" method with 10 recovery cycles, employing 0.5% trifluoroacetic acid (TFA) as the regeneration solution and 50 mM NH_4HCO_3 as the deposition solution. After which, all recovered solutions were combined, dried under nitrogen, redissolved in methanol, and centrifuged. The supernatant was filtered and transferred to a liquid chromatography vial.

2.6. UPLC-Q-TOF-MS/MS Analysis and Affinity Validation

The recovered samples from Section 2.5 and the corresponding *Psoralea corylifolia* extracts (dried and adjusted to 100 mg/mL in methanol) were analyzed using Acquity UPLC H-Class Plus Xevo Tof (Waters, USA). Chromatographic conditions were as follows: Mobile phase A was 0.1% formic acid in water; mobile phase B was 0.1% formic acid in acetonitrile; gradient elution: 0-0.5 min, 10% B; 0.5-1.0 min, 10%-70% B; 1.0-4.5 min, 70%-100% B; 4.5-5.5 min, 100% B; 5.5-6.5 min, 100%-10% B; 6.5-7.0 min, 10% B. Column temperature was maintained at 30 °C, flow rate adjusted to 0.3 mL/min, and injection volume set to 1 μL. Following the analysis, compounds in *Psoralea corylifolia* extracts that potentially bind to STAT3 protein were identified using Progenesis QI software by querying the ChemSpider Data Sources database for chemical information.

Psoralen and isopsoralen were separately diluted using the running buffer to generate multiple concentration gradients. These gradient samples were then employed to assess the binding affinity for STAT3 proteins, as described in section 2.3.

2.7. Molecular Docking Analysis

To investigate the potential specific binding of candidate small molecules to the active site of the STAT3 protein, molecular docking was employed to assess the interactions of psoralen and isopsoralen with the SH2 domain of STAT3. The SH2 domain serves as a dimerization module and key binding site for numerous non-peptidyl STAT3 inhibitors. It functions as a critical adaptor protein, facilitating STAT3 dimerization upon activation, mediating interactions between activated receptors and downstream signaling molecules, thereby promoting pathway activation. This signaling cascade plays a critical role in the pathogenesis of NSCLC. Therefore, the SH2 domain of STAT3 was selected as the target for molecular docking with the candidate ligands (psoralen and isopsoralen) and the established STAT3 SH2 inhibitor, Stattic (used as a positive control).

The crystal structure of STAT3 was obtained from the Protein Data Bank under accession ID 1BG1. Optimization was performed using Discovery Studio 2019 Client (DS) software to remove DNA strands and water molecules, and the STAT3-SH2 domain (residues 586-685) was selected as the docking site, with a 10 Å radius. The molecular structures of the two candidate compounds, statticin and isostatticin, were obtained from the Traditional Chinese Medicine Systematic Pharmacology Database and Analysis Platform (TCMSP). Protein-receptor docking was carried out

 doi:10.20944/preprints202512.1925.v1

using the CDOCKER module in DS software. Stattic was used as a positive control alongside the candidate compounds, and the optimal conformation was determined by CDOCKER binding energy.

2.8. A549 Cell Proliferation Assay

A549 cells in log-phase growth were plated into 96-well plates at a density targeted to reach approximately 70–80% confluence overnight. Candidate compounds at concentrations of 0, 10, 25, 50, 100, and 200 μmol/L were added to the A549 cells. 10 μL of the corresponding drug solution was added per well, and the plates were incubated for 24 h. After incubation, the medium was discarded, and 90 μL of fresh medium, along with 10 μL of 3-(4,5-dimethylthiazol-2-yl)-2,5-diphenyltetrazolium bromide (MTT) solution (5 mg/mL), was added to each well. The plate was incubated for four hours. The medium was subsequently discarded, and 100 μL of crystal violet dissolving solution was added to each well. The plates were shaken for 15 min. and absorbance was measured at 570 nm using a microplate reader (Biotek, USA).

2.9. A549 Cell Scratch Experiment

The cell scratch assay was used to evaluate the effect of candidate compounds on A549 cell migration. Log-phase A549 cells were seeded in 6-well plates to attain 90–100% confluence by the following day. Using a marker pen and a straightedge, lines were scribed on the plate surface. Wounds were created by scratching with a P200 pipette tip to ensure uniformity. The wells were then washed twice with PBS. Subsequently, the drug solution was added at a concentration near the IC_{50} (as determined from the MTT experiment). The cells were treated with STAT3 small-molecule inhibitors and incubated. Images were captured at 0, 24, and 48 h of culture using a fluorescence inverted microscope (Leica, Germany), and the cell migration rate was calculated based on wound closure.

2.10. Hydroxyl Radical Scavenging Capacity Assay

The salicylic acid method was used to determine the hydroxyl radical scavenging capacity of candidate compounds. Add 50 μL of 100 μM psoralen or isopsoralen, 50 μL of 6 mM ferrous sulfate ($FeSO_4$), and 50 μL of 6 mM hydrogen peroxide (H_2O_2) into a 96-well plate. The reaction mixture was mixed thoroughly for 10 min at room temperature. Subsequently, 50 μL of 6 mM salicylic acid was added to ethanol and incubated at room temperature for 30 min, avoiding light. The absorbance was measured at 510 nm, and the value was recorded as A_1. For the controls, the assay was performed identically; however, the sample was replaced with water to determine the absorbance value (recorded as A_0), and the H_2O_2 solution was replaced with water to determine the absorbance value (recorded as A_2). The clearance rate was calculated following the formula:

$$\text{Hydroxyl radical scavenging rate (\%)} = [1 - (A1 - A2) / A0] \times 100 \quad (1)$$

2.11. Superoxide Anion Scavenging Capacity Assay

The superoxide anion scavenging capacity of psoralen and isopsoralen was quantified using a modified pyrogallol autoxidation assay. One hundred μL of 100 μM psoralen or isopsoralen solution was thoroughly mixed with 450 μL of Tris-HCl buffer (0.1 M, pH 8.2) and maintained at room temperature for 20 min. Then, 50 μL of 2.5 M pyrogallol was added to initiate the reaction. After 5 min of reaction, 100 μL of 0.8 M HCl was added immediately to terminate the process. Absorbance was subsequently measured at 325 nm and recorded as A_1. For control experiments, a blank control (A_0) was prepared by replacing the sample solution with an equal volume of water, and a background control (A_2) was prepared by replacing the pyrogallol solution with an equal volume of water. The clearance rate was calculated following the formula:

$$\text{Superoxide anion scavenging rate (\%)} = [1 - (A_1 - A_2) / A_0] \times 100 \quad (2)$$

2.12. Intracellular ROS Level Assay

 doi:10.20944/preprints202512.1925.v1

Intracellular ROS levels were measured following treatment of human umbilical vein endothelial cells (HUVECs) and A549 cells with the candidate compounds to assess their effects and potential selectivity against H_2O_2 stress. HUVECs and A549 cells were plated separately in 96-well black plates. Following overnight culture, cells in the experimental groups were treated with serum-free medium containing 100 μM of either psoralen or isopsoralen. After 24 h of incubation, cells were washed with PBS. Then, cells from both experimental and control groups were exposed to serum-free medium supplemented with 500 μM H_2O_2 for four hours to induce oxidative stress. Intracellular ROS were then labeled with DCFH-DA, as instructed in the manufacturer's ROS assay kit. Fluorescence was subsequently measured using a fluorescence microplate reader.

2.13. HUVECs Cytotoxicity Assay

HUVECs in log-phase growth were plated in 96-well plates at 1.5×10^4 cells/well, with six replicate wells designated for each experimental group. After culturing for 24 h, the culture medium was carefully aspirated and replaced with 100 μL of fresh medium containing candidate compounds at 500 μmol/L, and the culture was incubated for an additional 24 h. Subsequently, 10 μL CCK-8 solution was added to each well and incubated for 30 min before the optical density was measured at 450 nm.

2.14. RAW264.7 Cytotoxicity Assay

The murine macrophage cell line RAW264.7 in log phase was plated at 5×10^5 cells/well in 96-well culture plates. After a 24-h incubation, the culture medium was aspirated and replaced with 100 μL of fresh medium supplemented with test compounds (500 μM final concentration). After an additional 24-h treatment period, 10 μL CCK-8 solution was added to each well and incubated for 30 min before optical density was measured at 450 nm.

2.15. Statistical Analysis

Experimental data were expressed as mean ± SD. Statistical analyses were explicitly conducted with GraphPad Prism software. One-way ANOVA was used to compare groups, with $P < 0.05$ as the threshold for statistical significance; figures were created with Origin software.

3. Results

3.1. Coupling Results of STAT3 Protein

The optimal conditions for STAT3 immobilization on the CM5 chip were identified as 10 mM sodium acetate at pH 4.0 and a STAT3 concentration of 50 μg/mL. Under these conditions, the ligand coupling channel yielded a robust RU value of 12,000 RU (Figure 3A). This coupling level is adequate for subsequent experiments.

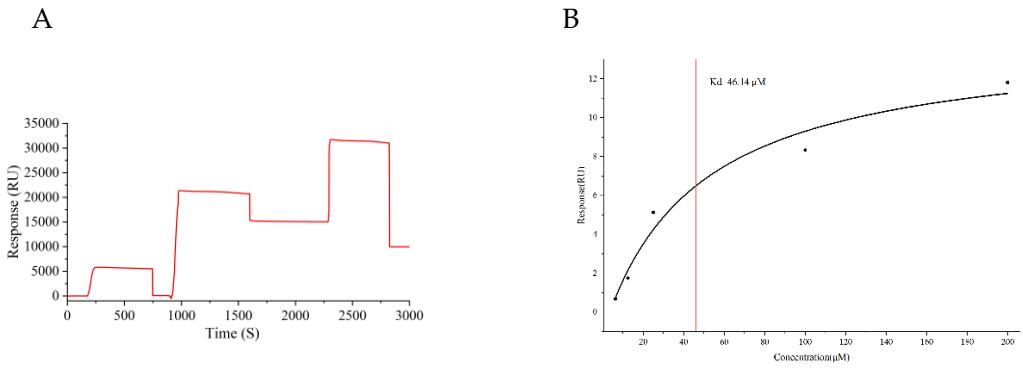

Figure 3. Sensor diagram of STAT3 protein immobilization onto the CM5 chip (**A**). The affinity constant between Stattic and STAT3 was 46.14 μM(**B**).

 doi:10.20944/preprints202512.1925.v1

3.2. Results of STAT3 Protein Chip Specificity Examination

Affinity analysis revealed a KD of 46.14 μM for Stattic with the STAT3 protein (Figure 3B). KD values are inversely correlated with binding affinity; lower KD values indicate stronger binding between a small molecule and its target protein. Typically, KD values for drug-grade small molecules binding to target proteins range from nM to μM. The KD value of 46.14 μM for Stattic in this study falls within this range. Therefore, Stattic can serve as a positive control for screening herbal compounds.

3.3. Ligand Screening of STAT3 Protein

According to SPR assays, both the 60% and 90% ethanol extracts of psoralen at 100 μg/mL showed binding activity to the STAT3 protein, with the 90% extract exhibiting stronger interaction (response values of 20.7 RU and 24.1 RU, respectively). It is generally accepted that a response value exceeding 20 RU, after subtracting the reference channel [31], indicates binding. Further concentration-dependent experiments confirmed that the response values of the psoralen 90% ethanol extract increased with concentration on the protein chip (Figure 4). This behavior clearly indicates that the extract contains bioactive components that specifically bind to STAT3.

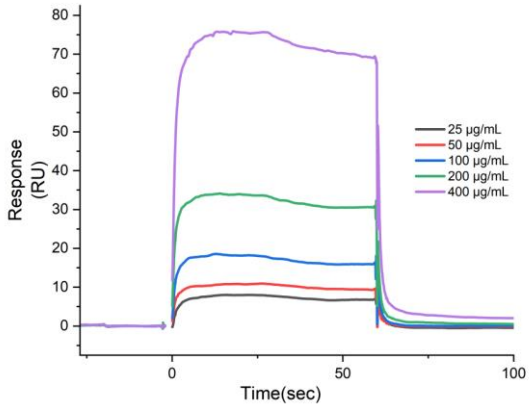

Figure 4. Binding response of 90% ethanol extract from *Psoralea corylifolia* to STAT3 protein.

3.4. UPLC-Q-TOF-MS/MS Analysis and Identification

The 90% ethanol extract of *Psoralea corylifolia* was injected into the SPR system using high-affinity coupling to STAT3 protein, aiming to recover the components enriched on the chip. UPLC-Q-TOF-MS/MS was used to analyze and identify both the extract and the recovered samples. The total ion chromatogram (TIC) of the recovered sample is shown in Figure 5A. The same ion signal peaks were identified in both the *Psoralea corylifolia* extract and its recovered sample, as shown in Figures 5B and 5C (Rt=2.94 min, m/z=187.0400 ([M+H]+)). The compound was queried as psoralen, and its tautomer, isopsoralen, was retrieved from the ChemSpider Data Sources database. The ion signal peaks of psoralen and isopsoralen standards under the same conditions are shown in Figure 5D (Rt=2.94 min, m/z=187.0400 ([M+H]+)). The detailed identification of the compounds is presented in Table 1.

A B

 doi:10.20944/preprints202512.1925.v1

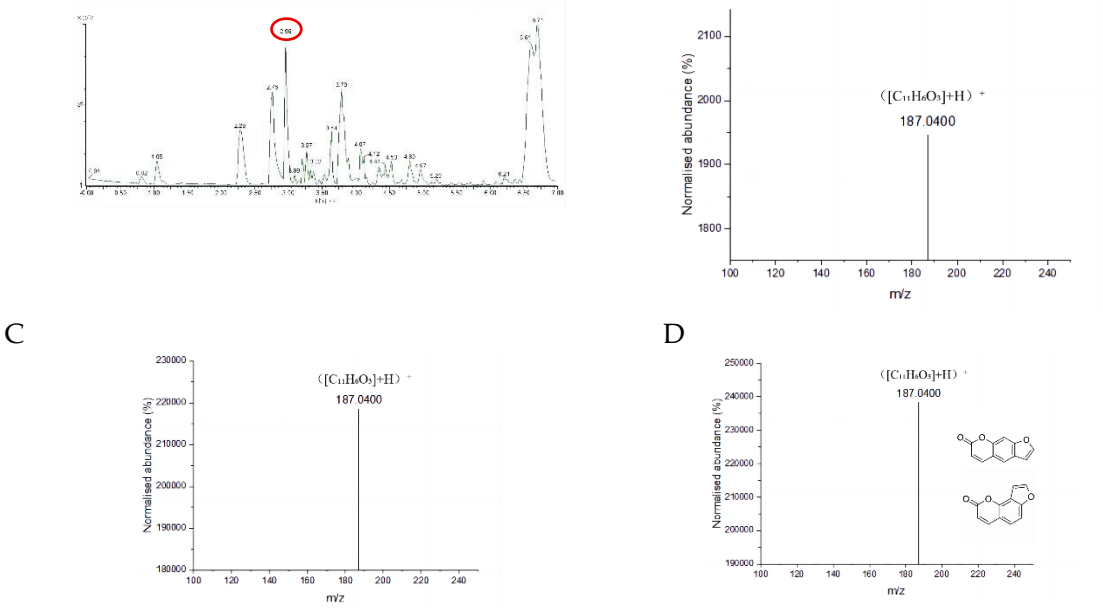

Figure 5. Total ion flow diagram of the recovered sample from *Psoralea corylifolia* (**A**), Mass spectra of *Psoralea corylifolia* (**B**), Mass spectra of recovered samples from *Psoralea corylifolia* (**C**), Mass spectra of psoralen and isopsoralen standards (**D**).

Table 1. Identification of chemical components from *Psoralea corylifolia.*

Serial Number	tR/min	Molecular Formula	Mass-to-charge Ratio (m/z)	Ion Mode	Error/ppm	Fragment Score	Compound
1	2.94	$C_{11}H_6O_3$	187.0400	M+H	5.7292	16.3	psoralen
2	2.94	$C_{11}H_6O_3$	187.0400	M+H	5.7292	16.3	isopsoralen

3.5. Validation of Affinity Between STAT3 Protein and Candidate Compounds

To verify whether psoralen and isopsoralen were bound to STAT3 protein, the affinity between both compounds and STAT3 was measured using a SPR assay. The results demonstrated stable, concentration-dependent binding signals between psoralen, isopsoralen, and STAT3 protein. The sensing signal graph and fitting curve for psoralen and STAT3 protein are depicted in Figure 6A, with a KD value of 80.92 μM, and those for isopsoralen and STAT3 protein are shown in Figure 6B, with a KD value of 28.11 μM. These results indicate that psoralen and isopsoralen bind specifically to STAT3.

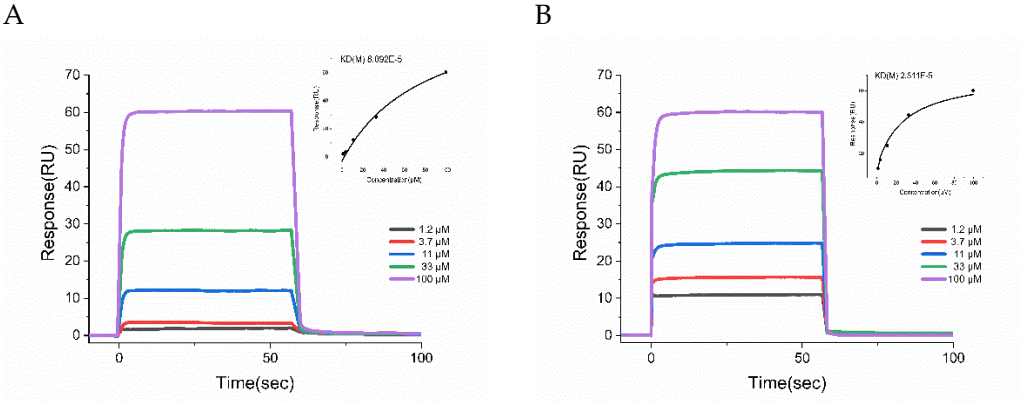

 doi:10.20944/preprints202512.1925.v1

Figure 6. The affinity constant between psoralen and STAT3 (**A**), and between isopsoralen and STAT3 (**B**).

3.6. Molecular Docking

The SH2 domain, a critical binding site for numerous non-peptide STAT3 inhibitors, contains three sub-pockets on its surface: the crucial phosphorylated Tyr705-specific binding pocket (pY pocket, residues Lys591, Arg609-620), the Leu706 subpocket (pY+1 pocket, residues 626-639), and the hydrophobic side pocket (pY-X pocket, residues 592-605), where the pY pocket exhibits the highest affinity [32]. Thus, the STAT3-SH2 domain protein (amino acid positions 586-685) was selected for docking with the candidate compounds and the positive control, Stattic.

The docking results of Stattic with the SH2 domain of STAT3 protein are presented in Figure 7A. Stattic forms hydrogen bonds with residues Lys591, Arg609, and Ser636, and alkyl hydrophobic interactions with Pro639, yielding a CDOCKER binding affinity of -23.494 kJ/mol. As shown in Figure 7B, psoralen forms cation-π interactions with Lys591, hydrogen bonds with Arg609, π-hydrophobic interactions with Val637, and alkyl hydrophobic interactions with Pro639, with a CDOCKER binding affinity of -18.6669 kJ/mol. Figure 7C shows the results for isopsoralen, which forms a cation-π interaction with Lys591, a hydrogen bond with Arg609, and an alkyl hydrophobic interaction with Pro639, resulting in a CDOCKER binding affinity of -20.9622 kJ/mol. Molecular docking reveals that both compounds establish strong hydrogen bonds within the pY pocket, indicating beneficial affinity for the SH2 domain of the STAT3 protein.

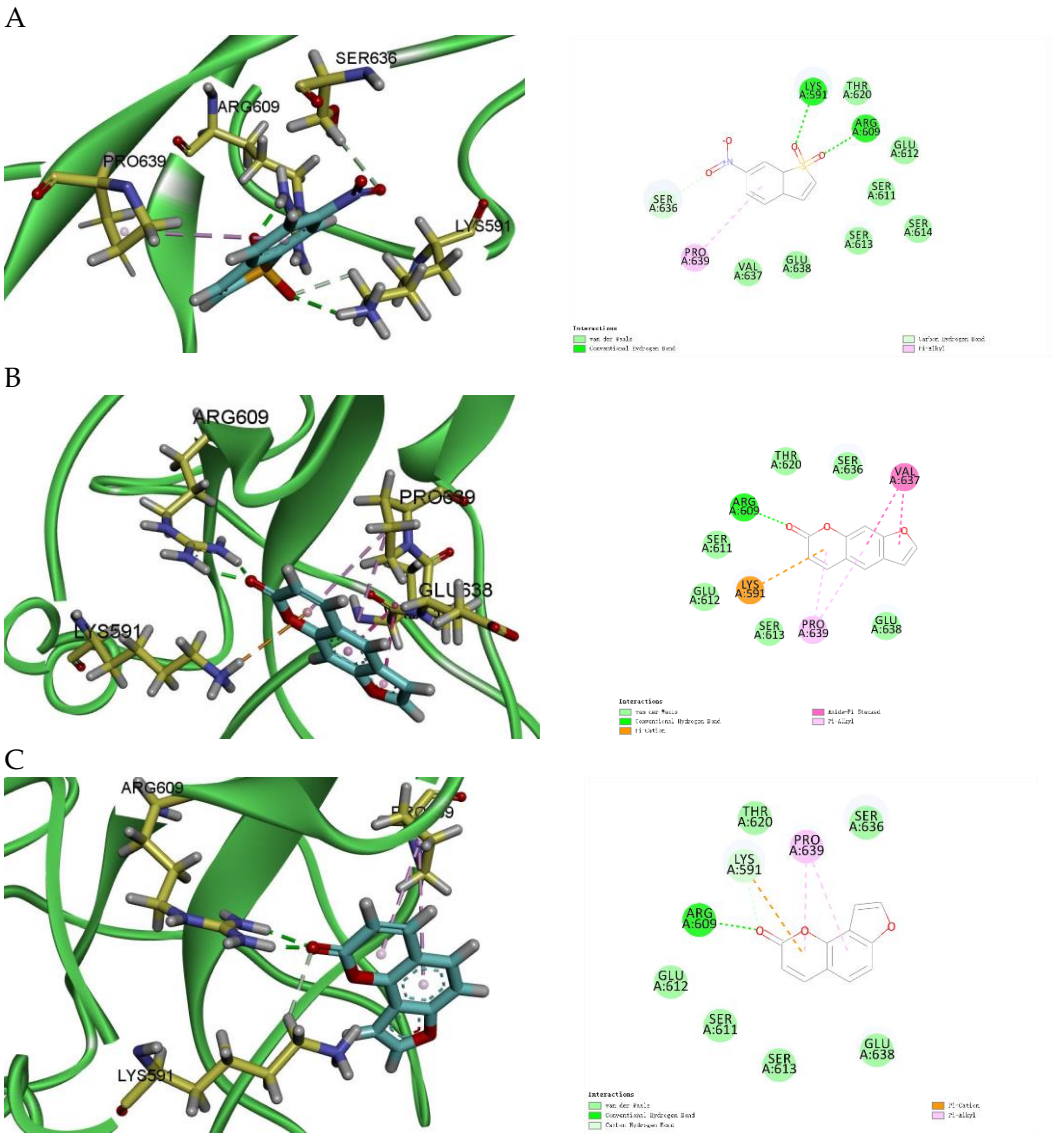

Figure 7. The interplay between the SH2 domain of STAT3 and Stattic (**A**) or psoralen (**B**), or isopsoralen (**C**).

 doi:10.20944/preprints202512.1925.v1

3.7. Proliferation Inhibitory Effects of Psoralen and Isopsoralen on A549 Cells

Different concentrations of the compounds (psoralen and isopsoralen) were applied to A549 cells. Absorbance values were measured to calculate cell survival rates, and IC_{50} values were 94.50 μmol/L for psoralen and 260.2 μmol/L for isopsoralen (Figure 8A-D). Results demonstrated that psoralen exhibited the most potent inhibitory effect among the compounds. Significant differences were also observed between treatment groups and the blank control group ($P < 0.01$), with cell survival rates decreasing in a concentration-dependent manner.

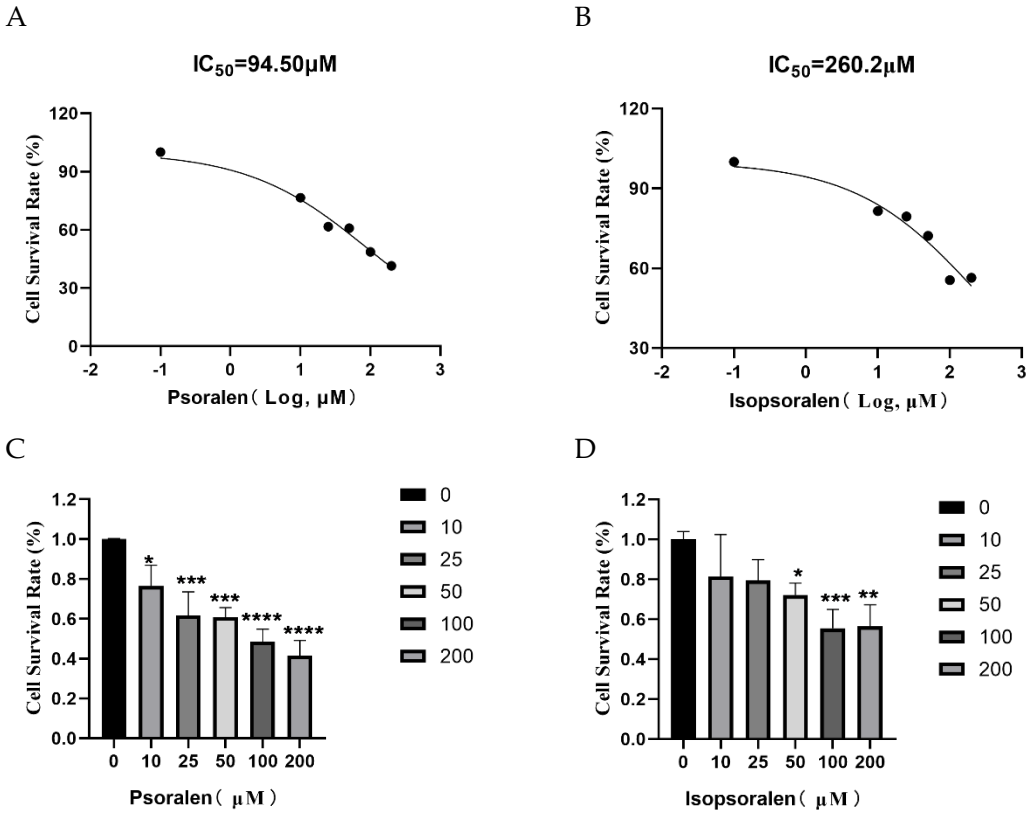

Figure 8. IC_{50} of psoralen (**A**) and isopsoralen (**B**) on A549 cell proliferation. Effects of varying concentrations of psoralen (**C**) and isopsoralen (**D**) on A549 cell proliferation.

3.8. The Inhibitory Effect of Psoralen and Isopsoralen on A549 Cell Migration using Scratch Assay

Based on MTT results, concentrations of 100 μM for psoralen and 200 μM for isopsoralen were selected. Migration areas were compared at 0, 24, and 48 h between the blank group and the treated groups. Images were captured at these time points, and migration rates were calculated using ImageJ software to determine significant differences. Results indicated that both compounds inhibited A549 cell migration (Figure 9A). At 24 h and 48 h, 200 μM isopsoralen showed the most significant inhibition ($P < 0.001$), while 100 μM psoralen was also found to have reduced migration rates (Figure 9B-C).

A

 doi:10.20944/preprints202512.1925.v1

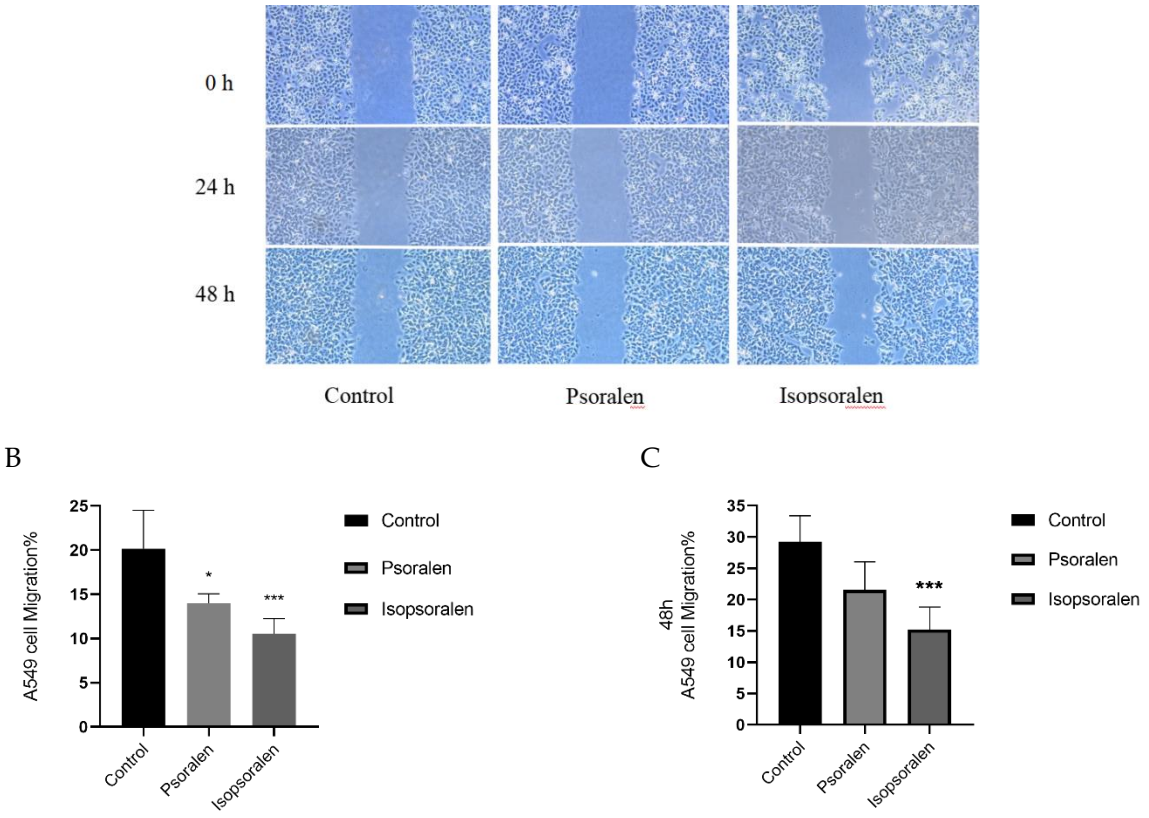

Figure 9. Inhibition of A549 cell migration by psoralen and isopsoralen (**A**), the effect of psoralen and isopsoralen treatment for 24 h(**B**) or 48 h (**C**) on the migration rate of A549 cells.

3.9. Extracellular Antioxidant Activity of Psoralen and Isopsoralen

As shown in Figure 10A, the hydroxyl radical scavenging assay using the salicylic acid method showed 82.44% and 76.04% scavenging rates for psoralens and isopsoralen, respectively, indicating potent hydroxyl radical scavenging activity for both compounds. Subsequently, in the superoxide anion scavenging assay (Figure 10B), psoralen demonstrated a scavenging rate of 29.43%, while isopsoralen showed a rate of 25.38%, highlighting their ability to eliminate superoxide anions effectively. These experimental findings confirm significant antioxidant properties in psoralen and isopsoralens.

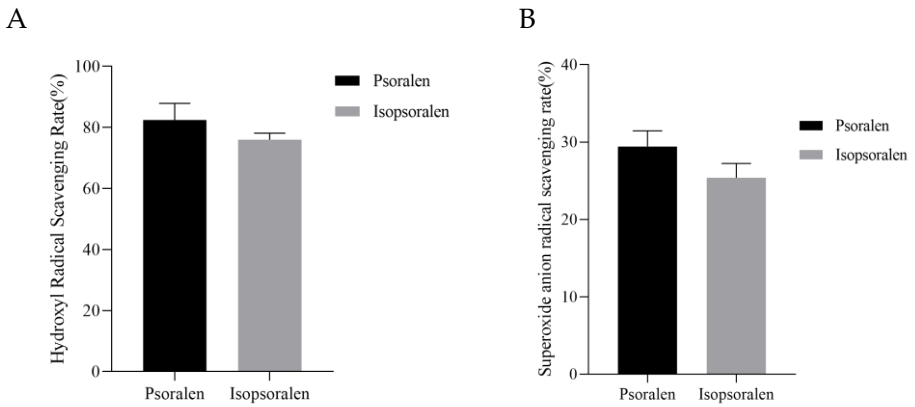

Figure 10. Scavenging rate of hydroxyl radicals (**A**) or superoxide anion radicals (**B**) by psoralen and isopsoralen.

3.10. Effects of Psoralen and Isopsoralen on Intracellular ROS Levels

The effects of psoralen and isopsoralen on ROS modulation were investigated in normal HUVECs (Figure 11A) and lung cancer A549 cells (Figure 11B). In a hydrogen peroxide-induced

 doi:10.20944/preprints202512.1925.v1

oxidative stress model, pretreatment with psoralen and isopsoralen significantly reduced ROS levels in HUVECs ($P < 0.01$), indicating a protective effect against oxidative stress. By contrast, pretreatment in A549 cells increased ROS levels ($P < 0.05$), intensifying ROS-mediated cellular damage and effectively inhibiting proliferative activity. This differential regulation suggests a bidirectional action for psoralen and isopsoralen: as ROS scavengers to mitigate oxidative injury in normal cells, but as promoters of ROS accumulation to enhance cytotoxicity in cancer cells. [29].

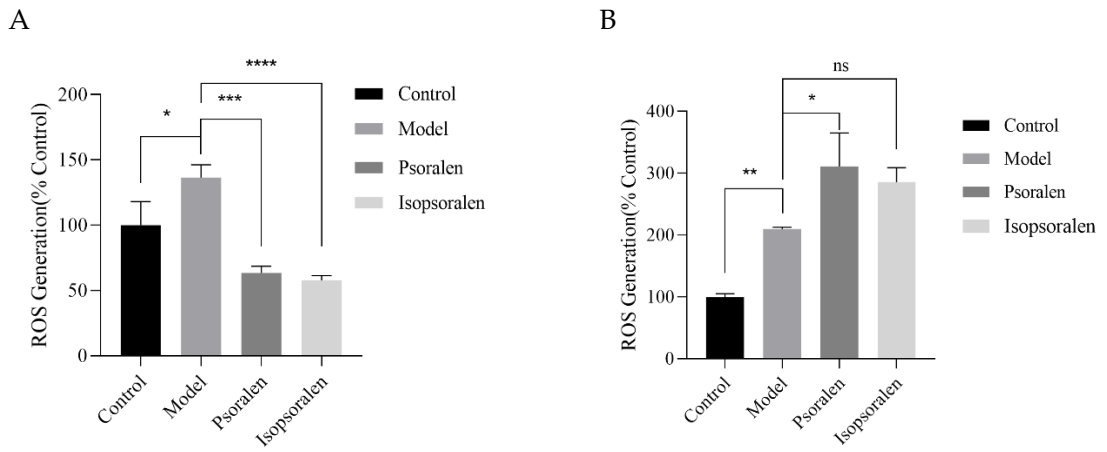

Figure 11. ROS levels in HUVECs (**A**) or A549 cells (**B**) in the oxidative stress model pretreated with psoralen and isopsoralen.

3.11. Effects of Psoralen and Isopsoralen on HUVECs Proliferation

HUVECs are primary cells isolated from umbilical cord veins and are sensitive to drugs, making them a standard tool for cytotoxicity testing. In this study, psoralen and isopsoralen were applied to HUVECs at 500 μmol/L to investigate their effects on normal cell proliferation (Figure 12A). Compared with the blank control group, neither psoralen nor isopsoralen at 500 μmol/L significantly affected HUVECs, indicating that neither compound was cytotoxic at this concentration.

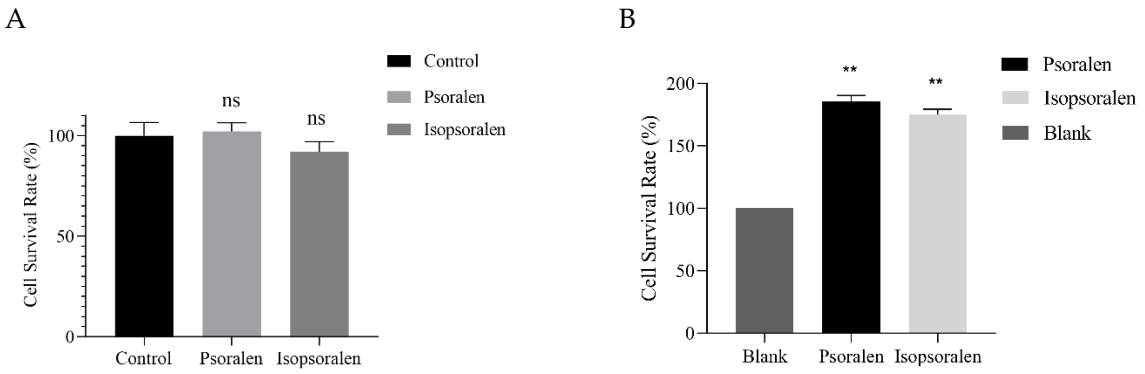

Figure 12. Effects of 500 μM psoralen and isopsoralen on the proliferation of HUVECs (**A**) or RAW264.7 cells (**B**).

3.12. Effects of Psoralen and Isopsoralen on RAW264.7 Cell Proliferation

RAW264.7 cells, commonly used to model human immune responses, were treated with 500 μmol/L of psoralen or isopsoralen. Compared to the control group, both compounds significantly increased the survival rate of RAW264.7 cells ($P < 0.01$), indicating that they promote proliferation rather than inhibit it (Figure 12B).

 doi:10.20944/preprints202512.1925.v1

4. Discussion

In this study, for the first time, the STAT3-specific small-molecule inhibitors psoralen and isopsoralen from *Psoralea corylifolia* were identified, using SPR-AIRS technology. These compounds effectively inhibited the proliferation and migration of NSCLC A549 cells, exhibiting a selective anticancer profile and unique bidirectional regulation of cellular redox status.

STAT3, as a key transcription factor, plays a central role in the onset, progression, metastasis, drug resistance, and immune escape of NSCLC [33,34]. Its sustained activation (constitutive or aberrant) is an essential feature of NSCLC and is closely associated with poor prognosis and chemoresistance [10]. Therefore, targeted inhibition of the STAT3 signaling pathway is considered a promising therapeutic strategy for NSCLC. However, the development of efficient and specific direct STAT3 inhibitors remains a significant challenge [35].

SPR-AIRS technology provides an efficient and reliable screening platform for STAT3-targeted compounds [36]. It offers higher target specificity than traditional cellular phenotypic screening, enabling direct identification of active ingredients from complex herbal extracts and real-time verification of binding affinity. We first screened two specific STAT3 small-molecule inhibitors, psoralen and isopsoralen, from *Psoralea corylifolia*. SPR results demonstrated that both compounds bound STAT3 directly and efficiently. Molecular docking analysis further revealed that psoralen and isopsoralen explicitly bound to the SH2 domain of STAT3, a functional domain critical for dimerization and activation. This mechanism is similar to that of known STAT3 inhibitors (e.g., Stattic) [37], suggesting that psoralen and isopsoralen may inhibit STAT3 transcriptional activity by blocking its phosphorylation.

In traditional Chinese medicine, extracts and specific active ingredients (including psoralen and isopsoralen in this study) of *Psoralea corylifolia* have been reported to have potential antitumor activity [38]. However, most prior research predominantly examined either the extracts' broad impact or the compounds' effects on alternative targets. In this study, we demonstrated the potential of psoralen and isopsoralen as specific, direct STAT3 inhibitors and systematically elucidated their mechanisms of action by combining SPR, molecular modeling, and in vitro functional assays. Both compounds significantly inhibited the cell growth and migratory capacity of A549 lung carcinoma cells. Notably, psoralen exhibited a more potent anti-proliferative effect despite its lower STAT3 binding affinity compared to isopsoralen. This apparent discrepancy suggests the involvement of complementary mechanisms beyond direct STAT3 inhibition. One such mechanism is their differential modulation of intracellular ROS. Our data reveal a dual function: in normal HUVECs, both compounds acted as cytoprotective antioxidants by scavenging hydrogen peroxide-induced ROS. Conversely, in A549 cancer cells, they triggered significant ROS accumulation, exacerbating oxidative stress and suppressing proliferation. This cancer cell-specific pro-oxidant effect represents a promising therapeutic strategy for selectively inducing cytotoxicity in malignant cells while sparing normal tissues [39].

5. Conclusions

In conclusion, SPR-AIRS technology was innovatively applied to identify and confirm psoralen and isopsoralen as novel small-molecule inhibitors of STAT3 derived from *Psoralea corylifolia*. From target identification to functional validation, this study establishes psoralen and isopsoralen as multifaceted anti-cancer agents. Their activity stems from a combination of direct STAT3 interaction and context-dependent, bidirectional modulation of ROS. The differential redox regulation, acting as an antioxidant in normal cells but a pro-oxidant in cancer cells, underscores its selective anticancer mechanism. Future work should focus on in vivo validation and further elucidate the detailed signaling pathways downstream of STAT3 and ROS that are affected by these compounds.

Author Contributions: Methodology and data curation, Liwei Bi, Guangyi Chen; validation, Wanfen Liu, Jing Feng; resources, Zhenyuan Yao; data curation, Siyi Chen; composing original manuscript, Liwei Bi, Anastacio T. Cagabhion III; evaluating and revising, Yu-Wei Chang, Yunghusan Chen.

Funding: This research was funded by the Fujian Provincial Natural Science Foundation (No. 2023J011658), the Natural Science Foundation of Xiamen (No.3502Z202374041), and the Natural Science program of Xiamen Medical College, grant number (K2021-1).

Institutional Review Board Statement: NA.

Informed Consent Statement: NA.

Data Availability Statement: All original data and findings presented in this study are included within the article, and further inquiries may be directed to the corresponding author.

Acknowledgments: The authors gratefully acknowledge Qiliang Zuo for his technical guidance, Qing Wang for providing traditionnal medicine *Psoralea corylifolia*, Shanshan Zhu and Fei Qin for providing equipment and resources, Jingna Wu for providing HUVECs, and Cheng He of Bailaibobio Ltd. for the data visualization.

Conflicts of Interest: No conflicts of interest.

References

1. Bray, F.; Laversanne, M.; Sung, H.; Ferlay, J.; Siegel, R.L.; Soerjomataram, I.; Jemal, A. Global Cancer Statistics 2022: GLOBOCAN Estimates of Incidence and Mortality Worldwide for 36 Cancers in 185 Countries. CA. *Cancer J. Clin.* **2024**, *74*, 229–263, doi:10.3322/caac.21834.
2. Mohrherr, J.; Uras, I.Z.; Moll, H.P.; Casanova, E. STAT3: Versatile Functions in Non-Small Cell Lung Cancer. *Cancers* **2020**, *12*, 1107, doi:10.3390/cancers12051107.
3. Zhu, H.; Xu, Y.; Gao, H.; Fan, X.; Fan, M.; Zhao, K.; Yang, H.; Zhu, Z.; Wu, K. Long-term Outcome of Definitive Radiotherapy for Locally Advanced Non-small Cell Lung Cancer: A Real-world Single-center Study in the Pre-durvalumab Era. *Cancer Med.* **2024**, *13*, e70051, doi:10.1002/cam4.70051.
4. Tang, Y.; Wang, Y.; Wang, X.; Zhao, Z.; Cai, H.; Xie, M.; Jiang, X.; Zhang, L.; Cheng, J.; Yang, L.; et al. Acetylshikonin Exerts Anti-Tumor Effects on Non-Small Cell Lung Cancer through Dual Inhibition of STAT3 and EGFR. *Phytomedicine* **2022**, *101*, 154109, doi:10.1016/j.phymed.2022.154109.
5. Sui, H.; Xiao, S.; Jiang, S.; Wu, S.; Lin, H.; Cheng, L.; Ye, L.; Zhao, Q.; Yu, Y.; Tao, L.; et al. Regorafenib Induces NOX5-Mediated Endoplasmic Reticulum Stress and Potentiates the Anti-Tumor Activity of Cisplatin in Non-Small Cell Lung Cancer Cells. *Neoplasia* **2023**, *39*, 100897, doi:10.1016/j.neo.2023.100897.
6. Ni, Y.; Wu, S.; Wang, X.; Zhu, G.; Chen, X.; Ding, Y.; Jiang, W. Cucurbitacin I Induces Pro-death Autophagy in A549 Cells via the ERK-mTOR-STAT3 Signaling Pathway. *J. Cell. Biochem.* **2018**, *119*, 6104–6112, doi:10.1002/jcb.26808.
7. Lai, I.-C.; Lai, G.-M.; Chow, J.-M.; Lee, H.-L.; Yeh, C.-F.; Li, C.-H.; Yan, J.-L.; Chuang, S.-E.; Whang-Peng, J.; Bai, K.-J.; et al. Active Fraction (HS7) from Taiwanofungus Camphoratus Inhibits AKT-mTOR, ERK and STAT3 Pathways and Induces CDK Inhibitors in CL1-0 Human Lung Cancer Cells. *Chin. Med.* **2017**, *12*, 33, doi:10.1186/s13020-017-0154-9.
8. Lin, C.-C.; Yeh, H.-H.; Huang, W.-L.; Yan, J.-J.; Lai, W.-W.; Su, W.-P.; Chen, H.H.W.; Su, W.-C. Metformin Enhances Cisplatin Cytotoxicity by Suppressing Signal Transducer and Activator of Transcription–3 Activity Independently of the Liver Kinase B1–AMP-Activated Protein Kinase Pathway. *Am. J. Respir. Cell Mol. Biol.* **2013**, *49*, 241–250, doi:10.1165/rcmb.2012-0244OC.
9. Gharibi, T.; Babaloo, Z.; Hosseini, A.; Abdollahpour-alitappeh, M.; Hashemi, V.; Marofi, F.; Nejati, K.; Baradaran, B. Targeting STAT3 in Cancer and Autoimmune Diseases. *Eur. J. Pharmacol.* **2020**, *878*, 173107, doi:10.1016/j.ejphar.2020.173107.
10. Morelli, A.P.; Tortelli, T.C.; Mancini, M.C.S.; Pavan, I.C.B.; Silva, L.G.S.; Severino, M.B.; Granato, D.C.; Pestana, N.F.; Ponte, L.G.S.; Peruca, G.F.; et al. STAT3 Contributes to Cisplatin Resistance, Modulating EMT Markers, and the mTOR Signaling in Lung Adenocarcinoma. *Neoplasia* **2021**, *23*, 1048–1058, doi:10.1016/j.neo.2021.08.003.
11. Jin, H.-O.; Lee, Y.-H.; Park, J.-A.; Kim, J.-H.; Hong, S.-E.; Kim, H.-A.; Kim, E.-K.; Noh, W.C.; Kim, B.-H.; Ye, S.-K.; et al. Blockage of Stat3 Enhances the Sensitivity of NSCLC Cells to PI3K/mTOR Inhibition. *Biochem. Biophys. Res. Commun.* **2014**, *444*, 502–508, doi:10.1016/j.bbrc.2014.01.086.

12. Zhou, Y.; Peng, X.; Fang, C.; Peng, X.; Tang, J.; Wang, Z.; Long, Y.; Chen, J.; Peng, Y.; Zhang, Z.; et al. Histones Methyltransferase NSD3 Inhibits Lung Adenocarcinoma Glycolysis Through Interacting with PPP1CB to Decrease STAT3 Signaling Pathway. *Adv. Sci.* **2024**, *11*, 2400381, doi:10.1002/advs.202400381.
13. Zhao, Y.; Zhang, X.; Li, Y.; Li, Y.; Zhang, H.; Song, Z.; Xu, J.; Guo, Y. A Natural Xanthone Suppresses Lung Cancer Growth and Metastasis by Targeting STAT3 and FAK Signaling Pathways. *Phytomedicine* **2022**, *102*, 154118, doi:10.1016/j.phymed.2022.154118.
14. Dong, J.; Cheng, X.-D.; Zhang, W.-D.; Qin, J.-J. Recent Update on Development of Small-Molecule STAT3 Inhibitors for Cancer Therapy: From Phosphorylation Inhibition to Protein Degradation. *J. Med. Chem.* **2021**, *64*, 8884–8915, doi:10.1021/acs.jmedchem.1c00629.
15. Dinakar, Y.H.; Kumar, H.; Mudavath, S.L.; Jain, R.; Ajmeer, R.; Jain, V. Role of STAT3 in the Initiation, Progression, Proliferation and Metastasis of Breast Cancer and Strategies to Deliver JAK and STAT3 Inhibitors. *Life Sci.* **2022**, *309*, 120996, doi:10.1016/j.lfs.2022.120996.
16. Xu,M.H.; Meng,Y.L.; Wang,X.X.; Xu,H.X.; Wang,B.; Wang,W.M. Effect of baicalin on expression of fibrogenic factors TGF-β1,mmp2 and timp2 in tissue of mice with pulmonary fibrosis. *China Journal of Chinese Materia Medica* **2020**, *45*, 5738–5744, doi:10.19540/j.cnki.cjcmm.20200908.401.
17. Chen, L.; Lv, D.; Chen, X.; Liu, M.; Wang, D.; Liu, Y.; Hong, Z.; Zhu, Z.; Hu, X.; Cao, Y.; et al. Biosensor-Based Active Ingredients Recognition System for Screening STAT3 Ligands from Medical Herbs. *Anal. Chem.* **2018**, *90*, 8936–8945, doi:10.1021/acs.analchem.8b01103.
18. Chen, L.; Chen, S.; Sun, P.; Liu, X.; Zhan, Z.; Wang, J. Psoralea Corylifolia L.: A Comprehensive Review of Its Botany, Traditional Uses, Phytochemistry, Pharmacology, Toxicology, Quality Control and Pharmacokinetics. *Chin. Med.* **2023**, *18*, 4, doi:10.1186/s13020-022-00704-6.
19. Shi, P.; Wang, L.; Qiu, X.; Yu, X.; Hayakawa, Y.; Han, N.; Yin, J. The Flavonoids from the Fruits of Psoralea Corylifolia and Their Potential in Inhibiting Metastasis of Human Non-Small Cell Lung Cancers. *Bioorganic Chem.* **2024**, *150*, 107604, doi:10.1016/j.bioorg.2024.107604.
20. Fan, Y.; Yin, L.; Zhong, X.; He, Z.; Meng, X.; Chai, F.; Kong, M.; Zhang, Q.; Xia, C.; Tong, Y.; et al. An Integrated Network Pharmacology, Molecular Docking and Experiment Validation Study to Investigate the Potential Mechanism of Isobavachalcone in the Treatment of Osteoarthritis. *J. Ethnopharmacol.* **2024**, *326*, 117827, doi:10.1016/j.jep.2024.117827.
21. Shi, Z.; Gao, J.; Pan, J.; Zhang, Z.; Zhang, G.; Wang, Y.; Gao, Y. A Systematic Review on the Safety of Psoraleae Fructus: Potential Risks, Toxic Characteristics, Underlying Mechanisms and Detoxification Methods. *Chin. J. Nat. Med.* **2022**, *20*, 805–813, doi:10.1016/S1875-5364(22)60234-6.
22. Chopra, B.; Dhingra, A.K.; Dhar, K.L. Psoralea Corylifolia L. (Buguchi) — Folklore to Modern Evidence: Review. *Fitoterapia* **2013**, *90*, 44–56, doi:10.1016/j.fitote.2013.06.016.
23. Wang, Y.; Hong, C.; Zhou, C.; Xu, D.; Qu, H. Screening Antitumor Compounds Psoralen and Isopsoralen from *Psoralea Corylifolia* L. Seeds. *Evid. Based Complement. Alternat. Med.* **2011**, *2011*, 363052, doi:10.1093/ecam/nen087.
24. Wang, X.; Xu, C.; Hua, Y.; Cheng, K.; Zhang, Y.; Liu, J.; Han, Y.; Liu, S.; Zhang, G.; Xu, S.; et al. Psoralen Induced Cell Cycle Arrest by Modulating Wnt/β-Catenin Pathway in Breast Cancer Cells. *Sci. Rep.* **2018**, *8*, 14001, doi:10.1038/s41598-018-32438-7.
25. Wang, X.; Peng, P.; Pan, Z.; Fang, Z.; Lu, W.; Liu, X. Psoralen Inhibits Malignant Proliferation and Induces Apoptosis through Triggering Endoplasmic Reticulum Stress in Human SMMC7721 Hepatoma Cells. *Biol. Res.* **2019**, *52*, 34, doi:10.1186/s40659-019-0241-8.
26. Li, K.; Zheng, Q.; Chen, X.; Wang, Y.; Wang, D.; Wang, J. Isobavachalcone Induces ROS-Mediated Apoptosis via Targeting Thioredoxin Reductase 1 in Human Prostate Cancer PC-3 Cells. *Oxid. Med. Cell. Longev.* **2018**, *2018*, 1915828, doi:10.1155/2018/1915828.
27. Sun, C.; Zhao, L.; Wang, X.; Hou, Y.; Guo, X.; Lu, J.; Chen, X. Psoralidin, a Natural Compound from *Psoralea Corylifolia* , Induces Oxidative Damage Mediated Apoptosis in Colon Cancer Cells. *J. Biochem. Mol. Toxicol.* **2022**, *36*, e23051, doi:10.1002/jbt.23051.
28. Lv, L.; Liu, B. Anti-Tumor Effects of Bakuchiol on Human Gastric Carcinoma Cell Lines Are Mediated through PI3K/AKT and MAPK Signaling Pathways. *Mol. Med. Rep.* **2017**, *16*, 8977–8982, doi:10.3892/mmr.2017.7696.

 doi:10.20944/preprints202512.1925.v1

29. Hao, W.; Zhang, X.; Zhao, W.; Chen, X. Psoralidin Induces Autophagy through ROS Generation Which Inhibits the Proliferation of Human Lung Cancer A549 Cells. *PeerJ* **2014**, *2*, e555, doi:10.7717/peerj.555.
30. Kumar, S.; Clair, D.St. Radioresistance in Prostate Cancer: Focus on the Interplay between NF-κB and SOD. *Antioxidants* **2021**, *10*, 1925, doi:10.3390/antiox10121925.
31. Ranbhise, J.S.; Singh, M.K.; Ju, S.; Han, S.; Yun, H.R.; Kim, S.S.; Kang, I. The Redox Paradox: Cancer's Double-Edged Sword for Malignancy and Therapy. *Antioxidants* **2025**, *14*, 1187, doi:10.3390/antiox14101187.
32. Kulkarni, V.V.; Wang, Y.; Pantaleon Garcia, J.; Evans, S.E. Redox-Dependent Activation of Lung Epithelial STAT3 Is Required for Inducible Protection against Bacterial Pneumonia. *Am. J. Respir. Cell Mol. Biol.* **2023**, *68*, 679–688, doi:10.1165/rcmb.2022-0342OC.
33. Hu, Y.; Dong, Z.; Liu, K. Unraveling the Complexity of STAT3 in Cancer: Molecular Understanding and Drug Discovery. *J. Exp. Clin. Cancer Res.* **2024**, *43*, 23, doi:10.1186/s13046-024-02949-5.
34. Shiah, J.V.; Grandis, J.R.; Johnson, D.E. Targeting STAT3 with Proteolysis Targeting Chimeras and Next-Generation Antisense Oligonucleotides. *Mol. Cancer Ther.* **2021**, *20*, 219–228, doi:10.1158/1535-7163.MCT-20-0599.
35. Li, S.; Wang, X.; Huang, J.; Cao, X.; Liu, Y.; Bai, S.; Zeng, T.; Chen, Q.; Li, C.; Lu, C.; et al. Decoy-PROTAC for Specific Degradation of "Undruggable" STAT3 Transcription Factor. *Cell Death Dis.* **2025**, *16*, 197, doi:10.1038/s41419-025-07535-x.
36. Lv, D.; Xu, J.; Qi, M.; Wang, D.; Xu, W.; Qiu, L.; Li, Y.; Cao, Y. A Strategy of Screening and Binding Analysis of Bioactive Components from Traditional Chinese Medicine Based on Surface Plasmon Resonance Biosensor. *J. Pharm. Anal.* **2022**, *12*, 500–508, doi:10.1016/j.jpha.2021.11.006.
37. Kasembeli, M.M.; Kaparos, E.; Bharadwaj, U.; Allaw, A.; Khouri, A.; Acot, B.; Tweardy, D.J. Aberrant Function of Pathogenic STAT3 Mutant Proteins Is Linked to Altered Stability of Monomers and Homodimers. *Blood* **2023**, *141*, 1411–1424, doi:10.1182/blood.2021015330.
38. Liu,G.T.;Gou,W.F.;Xu,F.F.;Guo J.H.;Wang,Y.F.;Li,W.L.;Hou,W.B. Research progress on antitumor mechanism of Psoraleae Fructus. *Chinese Traditional and Herbal Drugs* **2024**, *55*, 3529–3538.
39. Glorieux, C.; Liu, S.; Trachootham, D.; Huang, P. Targeting ROS in Cancer: Rationale and Strategies. *Nat. Rev. Drug Discov.* **2024**, *23*, 583–606, doi:10.1038/s41573-024-00979-4.